



# Fatigue S-N curves of bolts and bolted connections for application in civil engineering structures

Johan Maljaars<sup>a,b,\*</sup>, Mathias Euler<sup>c</sup>

<sup>a</sup> Eindhoven University of Technology, Groene Loper 3, Eindhoven, the Netherlands

<sup>b</sup> TNO, Stieltjesweg 1, Delft, the Netherlands

<sup>c</sup> Brandenburg University of Technology, Institute for Construction Engineering, Cottbus - Senftenberg, Germany

## ARTICLE INFO

### Keywords:

Fatigue tests  
Bolts  
Bolted connections  
Effect of preload  
Effect of hole forming  
EN 1993-1-9

## ABSTRACT

Bolts and bolted connections are frequently used in civil engineering steel structures. This paper presents a meta study where a few thousand fatigue tests on these elements are evaluated. The evaluation reveals that current specifications in design standards need updating to account for the relevant stress parameter and production methods. This substantially reduces the scatter of the fatigue resistance. The shape and position of the fatigue resistance (S-N) curves also require updating. The results of this study have been implemented in the new revision of European standard EN 1993-1-9. This paper provides the background for the modifications.

## 1. Introduction

Bolts and bolted connections are frequently applied in civil engineering structures such as bridges, crane supporting structures, masts, towers and chimneys. If carefully produced, some of these connections may have a better performance in fatigue as compared to welded connections. Design standards and recommendations provide FAT classes for the design of such products and connections. The FAT class refers to the 95% exceedance fraction of the fatigue resistance in [MPa] at two million cycles that can be used in the design.

Table 1 presents the FAT classes of bolts and of the most frequently applied bolted connections in three (inter) nationally used design standards, namely the American Bridge Design Specifications AASHTO:2012 [1], the European Standard EN 1993-1-9:2005 [2] and the British Standard BS 7608:2014 [3]. Double Covered Connections are abbreviated to DCC in this table. In all cases, a linear relationship is assumed between the logarithm of the applied stress range and the logarithm of the number of cycles to failure in the finite life region. The slope parameter is  $m = 3$  for all [1,2] or most [3] details, i.e. an endurance equivalent to the reciprocal of the stress range to the power of three.

Fatigue test data have been collected and evaluated for updating the FAT classes in the revision process of the European standard EN 1993-1-9. Thousands of test data have been collected, of which almost two thousand are considered relevant for civil engineering structures and are used to derive FAT classes. This meta study has resulted in substantial

modifications of the FAT classes, of the slope parameter, and for some details of the definition of the relevant stress for fatigue based on new insights obtained by this evaluation. This paper presents the background of the newly derived FAT classes.

## 2. Evaluation procedure

### 2.1. Selection of materials and production methods

Materials and production methods are selected that are typically used in civil engineering structures. Surface treatments such as polishing are usually not applied in this field. Mill scales were thus not removed in the specimens selected. An exception are DCC with preloaded high strength friction grip bolts, where a surface treatment such as blasting is applied at the contact surfaces, both in practice and in the selected specimens. Only full size specimens were selected, with plate thickness between  $9 \text{ mm} \leq t \leq 30 \text{ mm}$  and bolt diameters between  $12 \text{ mm} \leq D \leq 72 \text{ mm}$ .

The fatigue resistance may be correlated to the grade of steel. Some of the used sources report an increased fatigue resistance for steels of higher grade. Others, however, did not observe such an influence. Fig. 1 gives an illustrative example. The data from [4] for a 15 mm thick plate with an oxy-fuel cut hole shows no dependency on the steel grade (subfigure a), whereas the opposite is found for plasma cut holes (subfigure b). This is not necessarily related to the cutting process; the same authors did not find a consistent relation between fatigue resistance and

\* Corresponding author at: Eindhoven University of Technology, Groene Loper 3, Eindhoven, the Netherlands.

E-mail address: [johan.maljaars@tno.nl](mailto:johan.maljaars@tno.nl) (J. Maljaars).

Nomenclature	
<i>Abbreviations</i>	
6PRFLM	Six parameter random fatigue limit model
DCC	Double covered connection
DOF	Degree of freedom
FEM	Finite element method
FM	Fracture Mechanics
HDG	Hot-dip galvanized
HT/R	Bolts heat treated and then rolled
R/HT	Bolts rolled then heat treated
RO	Runout
SCF	Stress concentration factor
<i>Operators</i>	
^	Estimator
<i>Symbols</i>	
$\Delta\sigma_{C,M30}, \Delta\sigma_{C,M36}$	fatigue reference resistance at $N = 2 \cdot 10^6$ of a 30 or 36 mm diameter bolt
$\Delta\sigma_C$	fatigue reference resistance at $R = 0.5$ and $N = 2 \cdot 10^6$
$\Delta\sigma_{lim}$	Constant amplitude fatigue limit
$\Delta\sigma_{R,mod}$	Modified stress range at stress ratio $R$
$\Delta\sigma_{R,net}$	Net section stress range at stress ratio $R$
$\Delta\sigma_R$	Stress range at stress ratio $R$
$\Delta\tau_C$	Fatigue reference shear resistance at $N = 2 \cdot 10^6$
$\Delta\tau_R$	Range of average shear stress at stress ratio $R$
$\eta$	Stress ratio correction factor for Walker's equation
$\sigma'_f$	High cycle fatigue resistance in Morrow's equation
$\sigma_m$	Mean stress
$\sigma_{R,max}$	Maximum stress of a cycle with stress ratio $R$
$\sigma_u$	Tensile strength
$\sigma_y$	Yield stress
$\xi$	Stress ratio correction factor for Morrow's equation
$\zeta$	Stress ratio correction factor for Soderberg's equation
$a$	Constant in Basquin's relation
$a'$	Constant in the 6PRFLM
$b$	High cycle exponent in Morrow's equation
$c_1, c_2, c_3$	Coefficients in the SCF for DCC with non-preloaded bolts
$D$	Bolt diameter
$d_0$	Hole diameter
$f$	Confidence factor
$k$	Number of bolt rows per side of the connection
$K_f$	Fatigue notch factor
$k_n$	Prediction bound factor
$K_t$	Stress concentration factor
$K_t^{byp}$	Stress concentration factor for bypass loading
$K_t^{pin}$	Stress concentration factor for pin loading
$m$	Slope parameter in Basquin's relation
$m'$	Slope parameter in the 6PRFLM
$N$	Number of cycles to failure
$n$	Number of failed tests
$n_{RO}$	Number of run-out tests
$p$	Slope transition parameter in the 6PRFLM
$q$	Number of future samples
$R$	Stress ratio
$s$	Estimate of standard deviation of $\log(a)$
$t$	Plate thickness
$t_{0.05}$	5% coefficient of Student's T distribution
$w$	Ratio between plate width and number of bolts per row

steel grade for 15 mm thick plates with plasma cut edges in [5]. It is also not limited to thermal processes; different results regarding the influence of the steel grade are also reported for details such as DCC with preloaded bolts. Any influence of the steel grade may thus be depending on the production process and the type of detail, but it is not the entire explanation.

An important reason for these different observations may be in the surface quality of the specimens. Gurney [6] observed that the fatigue resistance increases with increasing tensile strength for plain machined specimen. In case of (sharply) notched specimen, the fatigue resistance did not increase with the tensile strength. The influence of the steel grade, if any, is also related to the mean stress of the cycle [7].

The fatigue resistance may thus benefit from a high steel grade in plain material and mechanically fastened connections in practical applications, provided that the specimen surface is relatively smooth. Given the treatment of materials during construction and use, an initially smooth product cannot always be guaranteed to remain smooth during the entire life without special provisions. Most civil engineering structures are currently constructed from steel grades with a nominal yield stress below 500 MPa. The S-N curves derived per detail in the following sections are therefore evaluated for steel grades with a nominal yield stress between 235 MPa  $\leq \sigma_y \leq$  460 MPa. This includes the European grades S235, S355 and S460, the American grades A36, A441 and A572, and equivalent steel grades. Data on higher steel grades are occasionally used to determine the influence of certain variations, such as the mean stress. Bolts are the exceptions, for which grades up to 10.9 (nominal yield stress of 900 MPa) have been considered.

Different observations have been reported on the influence of the zinc layer in Hot-Dip Galvanized (HDG) steel. Some authors show a clear reduction of the fatigue resistance of the detail types mentioned in the introduction [8,9] whereas others do not show a significant influence

[10,11]. One reason for these different observations is the thickness of the zinc layer; an influence is expected for a zinc layer exceeding a certain thickness [12], as the microcracks in the zinc layer are then deep enough to exceed the intrinsic threshold of the stress intensity factor range of the base metal. HDG steel is generally not considered in the current work, except for specific details and series where HDG test results are used to confirm a general trend in case the database of non galvanized samples was small. Details will be given in the subsequent sections. Bolts are again the exceptions, for which a separate evaluation was done on galvanized specimens.

### 2.2. Influence of the stress ratio

It is well known that the fatigue resistance of the considered constructional details depends on the mean stress. Three types of generally accepted and often applied mean stress corrections have been considered for comparing and pooling the fatigue test data that were carried out at different mean stress values,  $\sigma_m$ . The equations are generally applicable to tension-tension and tension-compression cycles (i.e. excluding compression-compression cycles).

The first mean stress correction is Morrow's correction on the Coffin-Manson relationship. The high-cycle fatigue part of the equation, considering stress ranges  $\Delta\sigma_R$  that remain in the linear elastic stage, reads:

$$\Delta\sigma_R = 2(2N)^b (\sigma'_f - \sigma_m) \tag{1}$$

where  $N$  is the number of cycles to failure and  $\sigma'_f$  and  $b$  are resistance parameters. If correcting the exponent  $b$  for the surface roughness of the mill scale according to [7] or [13], it appears that the fatigue resistance is almost independent of the material tensile strength around the fatigue

limit. Eq. (1) then results into the following stress ratio dependency:

$$\Delta\sigma_R = \Delta\sigma_0 \frac{1-R}{1-\xi R} \tag{2}$$

where  $R$  is the stress ratio according to Eq. (3),  $\Delta\sigma_R$  is the stress range at stress ratio  $R$  (hence  $\Delta\sigma_0$  is the stress range at  $R = 0$ ) and  $\xi = 1 - \Delta\sigma_0/\sigma'_f$ . The format of Eq. (2) is applied in many old German standards, such as [14] for riveted railway bridges, where  $\xi$  ranges between 0.4 and 0.6.

$$R = \frac{\sigma_m - 0.5\Delta\sigma_R}{\sigma_m + 0.5\Delta\sigma_R} \tag{3}$$

Soderberg [15] relates the fatigue resistance to the ratio between the applied mean stress and the material yield stress,  $\sigma_y$ :

$$\frac{\Delta\sigma_R}{\Delta\sigma_{-1}} + \frac{\sigma_m}{\sigma_y} = 1 \tag{4}$$

where the numerical subscript refers to the stress ratio (in this case  $R = -1$ ). The equation strictly applies to the constant amplitude fatigue limit but it is often considered as well for other stress ranges. The resulting equation can be written in a more general form as:

$$\Delta\sigma_R = \Delta\sigma_0 \frac{1-R}{1+R\left(\frac{\Delta\sigma_0}{\zeta\sigma_y} - 1\right)} \tag{5}$$

where  $\zeta = 1$  for Soderberg and  $\zeta = \sigma_{tu}/\sigma_y$  in case of Goodman [16], where  $\sigma_{tu}$  is the material tensile strength.

The Walker equation [17] assumes that the fatigue resistance is not

only depending on the stress range, but also on the maximum stress,  $\sigma_{R,max}$ . The Walker equation reads:

$$\Delta\sigma_R^{(1-\eta)} \sigma_{R,max}^\eta = \Delta\sigma_{-1}^{(1-\eta)} \sigma_{-1,max}^\eta \tag{6}$$

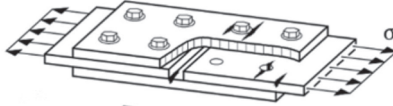
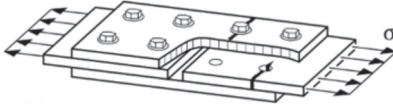
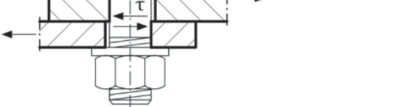
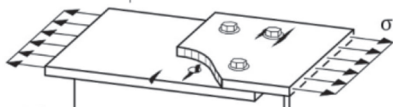
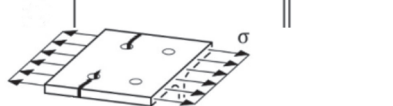
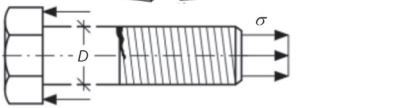
This equation is a generalised form of the Smith-Watson-Topper parameter [18] written in the shape of Langlas and Vogel [19], where  $\eta = 0.5$  in the high cycle range. Eq. (6) can be written as:

$$\Delta\sigma_R = \Delta\sigma_0(1-R)^\eta \tag{7}$$

Generally, a detail dependent Stress Concentration Factor (SCF) applies, which implies that  $\xi, \zeta,$  and  $\eta$  depend on the type of detail. All collected fatigue test data have a stress ratio ranging between  $-1 \leq R \leq 0.5$ . With the flexibility introduced by  $\xi, \zeta,$  and  $\eta$  and for the considered ranges of steel grade and stress ratio, Eq. (2), (5) and (7) can reasonably approximate other stress ratio dependencies, such as those of Goodman [16], Gerber [20] and Dietmann [21]. The dependency of Marin [22] deviates from the others and it cannot be approximated with reasonable accuracy by Eqs. (2), (5) and (7). These relationships in [16,20–22] make use of the tensile strength, however, some sources only give the nominal value or the measured yield stress.

The collected fatigue test data that will be presented in the following sections are evaluated for the best fit values of parameters  $\xi, \zeta,$  and  $\eta$  per type of detail. As an example, Fig. 2(a) provides the collected failed test data of DCC with preloaded high strength friction grip bolts, where the gross section of the specimen is used to calculate the stress range. Three of the series from [10] are displayed in colours. These are carried out at  $R = -0.6, R = 0$  and  $R = 0.5$  but the specimens are produced with identical material, surface and hole forming methods. Parameters  $\xi, \zeta,$  and  $\eta$  are determined using these three series such, that the scatter of the

**Table 1**  
FAT classes according to AASHTO:2012 [1], EN 1993-1-9:2005 [2] and BS 7608:2014 [3].

Detail	Figure	[1]	[2]	[3]
DCC with preloaded bolts, plate failure		125;71 <sup>a)</sup>	112	130
DCC non preloaded, plate failure, normal holes			50	52
DCC non preloaded, plate failure, fitted bolts			80	97
DCC non preloaded, bolt failure <sup>b)</sup>			100	104
Single lap connection, preloaded bolts, plate failure		125;71 <sup>a)</sup>	90	97
Element with holes		71	90	97;54 <sup>c)</sup>
Bolts in tension		40	50 <sup>d)</sup>	59 <sup>d)</sup>

<sup>a)</sup> FAT 125 for drilled or reamed holes, FAT 71 for punched holes.  
<sup>b)</sup> Shear stress in bolt shaft. Thread not in shear plane.  
<sup>c)</sup> FAT 97 for drilled or reamed holes, FAT 54 for thermally cut holes.  
<sup>d)</sup> Reduction of the FAT class for large diameter bolts in EN 1993-1-9 and BS 7608.

S-N curve is minimised. This gives  $\xi = 0.4$ ,  $\zeta = 1.1$ , and  $\eta = 0.6$ . These corrections are subsequently applied to all data collected on that detail. Fig. 2(b) provides the data for stress ranges corrected to a stress ratio of  $R = 0$  using Morrow's Eq. (2) with  $\xi = 0.4$ . The figure shows a substantial reduction of the scatter as compared to the original data. A similar result is obtained with Walker's Eq. (7) and  $\eta = 0.6$ . The scatter after stress ratio correction is larger in case of Soderberg's Eq. (5) with  $\zeta = 1.1$ . (Section 3.1 gives a further elaboration of this detail.) Similar evaluations are performed for the other types of detail and in most cases, Eqs. (2) and (7) give a similar remaining scatter and they outperform Eq. (5). For this reason, all data in the subsequent sections are corrected for the stress ratio using Eq. (2).

The stress ratio in most practical civil engineering structures ranges from very low to very high. However, for very high stress ratios, such as  $R > 0.5$ , the static resistance is often decisive for the steel grades and structure types described before. In addition, test data with  $R > 0.5$  are rare. For a safe fatigue design of general application, the fatigue resistance is therefore evaluated at a stress ratio of  $R = 0.5$  ( $\Delta\sigma_{0.5}$ ) in the subsequent sections. A separate evaluation is done for bolts loaded in tension, Section 3.5.

### 2.3. Statistical evaluation of test data

An S-N curve is derived for each dataset. The Basquin relationship is assumed between  $N$  and  $\Delta\sigma_{0.5}$ :

$$\log N = \log a - m \log \Delta\sigma_{0.5} \quad (8)$$

where parameters  $m$  and  $\log a$  are detail dependent and based on failed specimens only (i.e. excluding run-outs). They are derived for the 10-base-logarithm. It is assumed that  $\log a$  is normally distributed. The estimates of  $m$  and  $a$  based on the test data consisting of  $n$  failed tests are denoted  $\hat{m}$  and  $\hat{a}$ , respectively:

$$\hat{m} = \frac{-n \sum (\log \Delta\sigma_{0.5,i} \log N_i) + \sum \log \Delta\sigma_{0.5,i} \sum \log N_i}{n \sum (\log \Delta\sigma_{0.5,i})^2 - (\sum \log \Delta\sigma_{0.5,i})^2} \quad (9)$$

$$\hat{a} = \frac{1}{n} \left( \sum \log N_i + \hat{m} \sum \log \Delta\sigma_{0.5,i} \right) \quad (10)$$

The estimate of the standard deviation of  $\log a$  is denoted with  $s$ :

$$s = \sqrt{\frac{\sum (\log N_i - \log \hat{a} + \hat{m} \log \Delta\sigma_{0.5,i})^2}{\lambda}} \quad (11)$$

where  $\lambda$  is the Degree Of Freedom (DOF), quantified below. The

fatigue reference resistance, defined as the 95% lower prediction bound of the fatigue resistance at 2 million cycles and at a stress ratio of  $R = 0.5$ , is denoted as  $\Delta\sigma_C$ :

$$\log \Delta\sigma_C = \frac{(\log \hat{a} - \log(2 \cdot 10^6) - k_n s)}{\hat{m}} \quad (12)$$

where  $k_n$  is the prediction bound factor:

$$k_n = t_{0.05} \sqrt{\frac{1}{n} + \frac{1}{q} + f} \quad (13)$$

where  $t_{0.05}$  is the 5% coefficient of Student's T distribution with DOF equal to  $\lambda = n - 3$  (considering the three estimated parameters  $\hat{a}$ ,  $\hat{m}$  and  $\xi$ ),  $q$  is the number of future samples, which is taken as 1, and  $f$  is a factor considering the confidence of the prediction at the specific stress range  $\Delta\sigma_C$ , which is related to the relative difference between that stress range and the centre - or average stress range - of the data [23]:

$$f = \frac{\left( \frac{\log \hat{a} - \log(2 \cdot 10^6)}{\hat{m}} - \frac{1}{n} \sum \log \Delta\sigma_{0.5,i} \right)^2}{\sum \left( \log \Delta\sigma_{0.5,i} - \frac{1}{n} \sum \log \Delta\sigma_{0.5,i} \right)^2} \quad (14)$$

Sub-groups are defined for most of the details regarding the production method or geometry. The Kolmogorov-Smirnov test [24] is applied on the values of  $a$  per test to verify whether the subdivision into subgroups is justified. This statistical test indeed rejected the null hypothesis that the distinguished sub-groups belong to the same distribution for every defined sub-group.

In pooling data of series with (remaining) differences in material properties, surface smoothness, production process, geometry or stress ratio, the data fit with the Basquin relationship Eq. (8) may be worse than in case of an individual series. The nature of the Basquin relationship is such, that a worse fit results in a smaller value of  $\hat{m}$ . For this reason,  $\hat{m}$  is estimated for individual series, but only if the series covers at least 1.5 decades of  $N$  as a smaller coverage may lead to an inaccurate determination. The DOF increases to  $\lambda = n - 2$  because of the absence of  $\xi$  as a parameter in case of an individual series. The fatigue reference resistance  $\Delta\sigma_C$  (Eq. 12) is determined for all series pooled per sub-group of detail type and using fixed (prior) slope parameters  $m = 3$  and  $m = 5$ . The DOF is  $\lambda = n - 2$  in that case because  $m$  is taken as prior.

All data in the subsequent sections are presented in graphs with a maximum stress range 20 times larger than the minimum stress range on the ordinate, thereby enabling a visual comparison between the graphs.

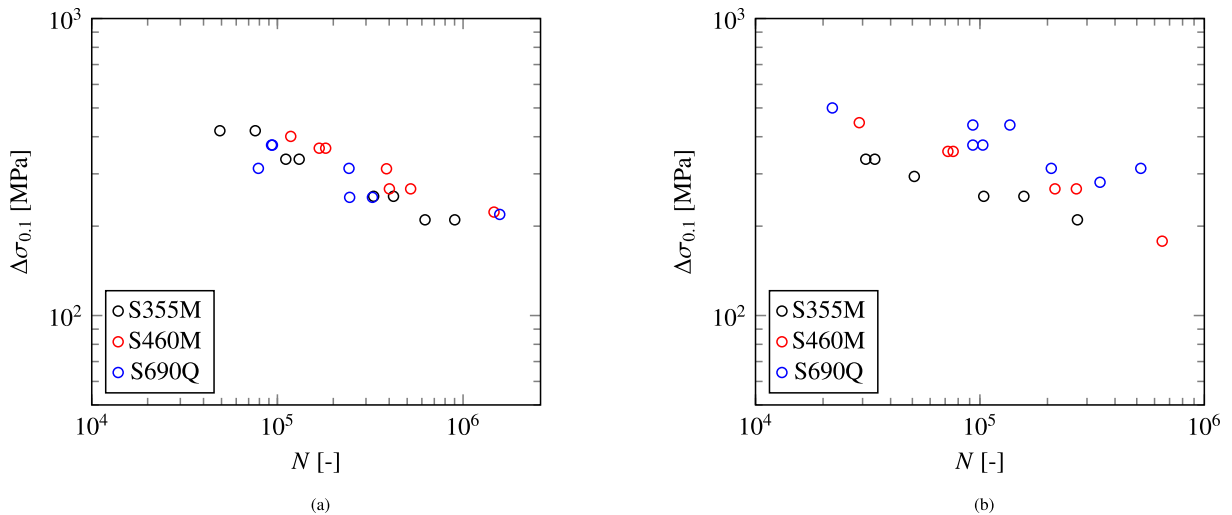


Fig. 1. Data from plates with cut holes at stress ratio  $R = 0.1$  from [4]: (a) Oxy-fuel cut holes; (b) Plasma cut holes.

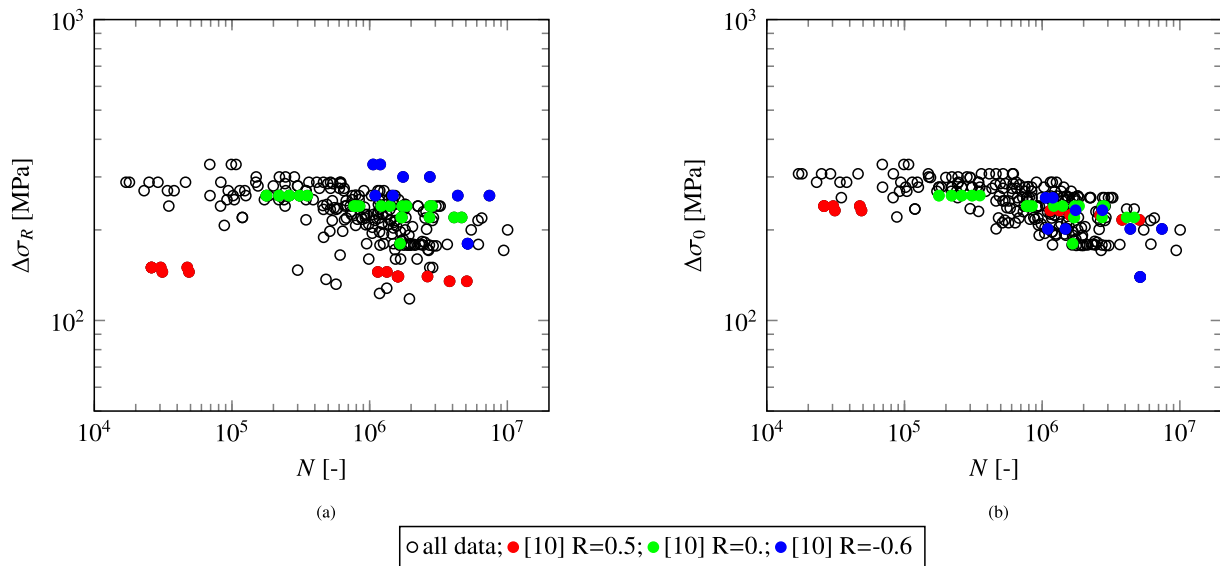


Fig. 2. Data for double covered connections (DCC) with preloaded bolts: (a) As-received; (b) Corrected to a stress ratio  $R = 0$ .

### 3. Test data per detail type

#### 3.1. Double covered connections (DCC) with preloaded bolts

It is well known that the load transfer in DCC depends on whether the bolts are preloaded [25]. The forces are transferred through friction between the plates in DCC with preloaded high strength friction grip bolts. The associated failure mode is then usually fretting fatigue at the end of the washer or sometimes at the end of the cover plate, as demonstrated among others by [26,27]. The plate surface treatment and preloading procedure should be subject to careful execution, or otherwise, the fatigue resistance may be significantly lower. As an example, fatigue cracks starting from the hole edge were observed in [28] and the fatigue resistance was significantly lower than that of other series. This was attributed to the oil used for drilling the holes, which has penetrated between the plates. Even in case of no apparent errors in the preloading procedure, cracks starting from the hole are occasionally reported.

Yin et al. [29] and Albrecht et al. [30] state that the fatigue resistance reduces as the number of bolt rows increases, because the frictional force transfer near the first bolt row is larger than that of the others. A fatigue resistance equal to that of a hole in a plate is reported for four (or more) rows of bolt per side of the connection. In contrast, tests in [31] with four bolt rows give a similar fatigue resistance as those with two bolt rows per side. The difference between these sources may be related to the safety against slip. These connections are usually designed for slip resistance under static loading, in which the resistance is determined as the summed preload forces of all bolts multiplied by the slip factor. In the weakest link failure mode of fatigue, it is the first bolt row that is decisive regarding slip force and bypass loading. The slip requirement may hence be stricter for fatigue as compared to the static failure mode in connections with a large number of bolt rows.

Table A.1 provides the series used in the statistical evaluation. Data are only considered for which the preload force and preload procedure are fully documented, in agreement with modern standards, and theoretically sufficient to prevent slip. The slope parameter of the individual series range between  $5.3 \leq \hat{m} \leq 51$  with an average of  $\hat{m} = 17$ . This is substantially higher than the slope parameters of the other detail types that will be discussed in subsequent sections. The data corrected to a stress ratio of  $R = 0$  were already presented in Fig. 2b. These data suggest that the S-N curve of the pooled data runs flatter at high stress ranges than at low stress ranges. Considering the data more closely, it appears that a significant number of the tests were carried out with the

maximum gross stress close to or even exceeding the yield stress. The applied stress is distributed between the main plate and the covered plates, however, it can result into a high Von Mises stress if combined with the compression stress in plate thickness direction caused by bolt preloading. Yielding may influence the fatigue resistance particularly for this detail, as it may alter the contact between the components. Fig. 3 presents the data again (with the gross stress range on the ordinate), but including RunOut tests (RO) and with the data corrected to a stress ratio of  $R = 0.5$ . Three subgroups are distinguished:

- The maximum stress of the cycle exceeds the yield stress (red dots).
- The maximum stress is between yield and 90% of yield (orange dots).
- The other data (black dots).

An additional series is added with a high yield stress (blue squares), which has a maximum ratio  $\sigma_{R,max}/\sigma_y$  of 0.45. The data show a clear influence of the ratio  $\sigma_{R,max}/\sigma_y$ . The higher this ratio, the flatter is the S-N curve. The data with  $\sigma_y \geq 827$  MPa are on the lower bound of the entire pool for endurance greater than  $2 \cdot 10^5$  cycles but they clearly exceed the resistance of other series for lower endurance. The statistical evaluation was performed without these high strength steel grades. The fatigue reference resistance for an assumed slope of  $m = 5$  increases from 81 MPa considering all (other) data to 84 MPa when excluding the data with  $\sigma_{R,max}/\sigma_y \geq 1$  and to 89 MPa when excluding the data with  $\sigma_{R,max}/\sigma_y \geq 0.9$ . Excluding these subgroups has a negligible influence on  $\xi$  and on  $\Delta\sigma_C$  for  $m = 17$ , which gives  $\Delta\sigma_C = 112$  MPa.

A few data at  $\sigma_{max}/\sigma_y < 0.9$  (near  $N = 10^5$  and at  $N = 5 \cdot 10^6$ ) are below the general trend. This may have been caused by unintended slip. As this may also occur in practice, these outliers have been included in the statistical evaluation.

The data in Fig. 3 include HDG steel series from [10]. They have been added because these data allow to evaluate  $\xi$  because of the large coverage of stress ratios. The non-galvanized data were all carried out between  $0 \leq R \leq 0.25$ . The HDG series at  $R = 0$  in [10] gave an average fatigue resistance that was 6% larger than that of the non-galvanized series of the same source and with the same stress ratio. Excluding the HDG series (but keeping  $\xi$ ) has no effect on the fatigue reference resistance of the entire database.

A special case is formed by DCC with preloaded injection bolts. Tests have shown that the resin does not fail in fatigue [32]. However, a (small) fraction of the load may be transferred through bearing in such a connection [32]. Only one source with fatigue tests was found on this

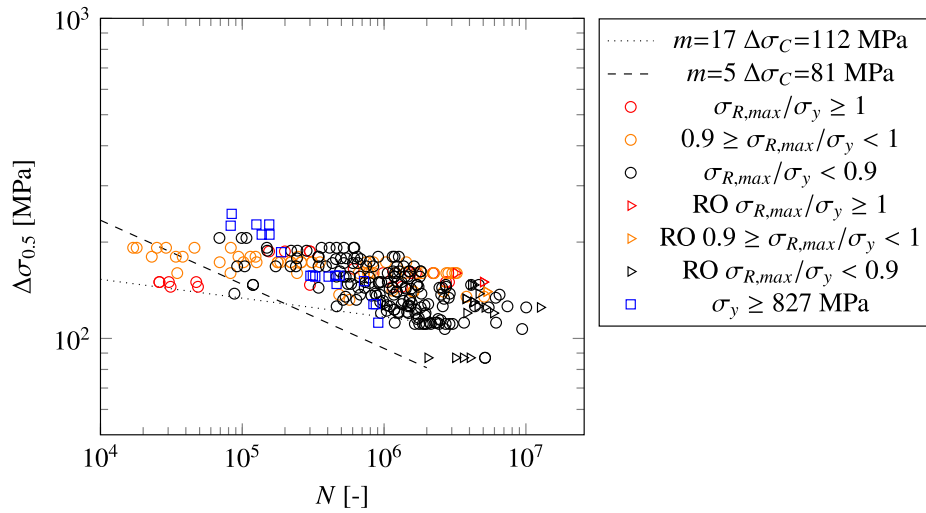


Fig. 3. Data for double covered connections (DCC) with preloaded high strength friction grip bolts, showing the influence of the maximum stress.

typical [33], where it was observed that the fatigue resistance with preloaded injection bolts was lower than that of normal preloaded high strength friction grip bolts.

### 3.2. Double covered connections (DCC) with non-preloaded bolts

The forces are transferred via shear of the bolts and bearing of the plates in DCC with non-preloaded bolts. Two potential failure modes apply in this case, namely, failure of the plate or failure of the bolt. In the first failure mode of plate failure, the largest stress concentration occurs at the hole and this is the location where cracks initiate. For this reason, data are usually evaluated using the net section stress range  $\Delta\sigma_{R,net}$ . Valtinat and Huhn [10] have demonstrated that the fatigue resistance of DCC with bolts with a small preload – not preventing slip – is larger than that of DCC with bolts without any preload. Therefore, test data are only included in the evaluation if the sources informed that the preload of the bolts was negligible, such as in snug-tight bolts or hand-turned nuts.

Table A.2 and Fig. 4(a) show the collected data. The slope parameters of the individual series ranged between  $4.3 < \bar{m} \leq 8.9$ , with an average value of 5.8. A large scatter results when pooling all data. The data with  $R = 0.3$  generally give a higher endurance than the data with higher

stress ratio but also those with lower stress ratios. This difference cannot be explained by a simple stress ratio correction alone. The scatter is believed to be (also) related to the differences in geometry. Therefore, this paper proposes a new definition of the stress range for this detail type, which is derived as follows: The geometry of the connection determines which fraction of the load is passing the hole (bypass loading) and which fraction is transferred through bearing with the bolt acting as a pin. The SCF-s for bypass and pin loading,  $K_t^{byp}$  and  $K_t^{pin}$  respectively, are different (Fig. 5):

$$K_t^{byp} = 2 + 0.284 \left(1 - \frac{d_0}{w}\right) - 0.6 \left(1 - \frac{d_0}{w}\right)^2 + 1.32 \left(1 - \frac{d_0}{w}\right)^3 \quad (15)$$

$$K_t^{pin} = 12.88 - 52.71 \frac{d_0}{w} + 89.76 \left(\frac{d_0}{w}\right)^2 - 51.67 \left(\frac{d_0}{w}\right)^3 \quad (16)$$

where  $d_0$  is the hole diameter and  $w$  is the plate width divided by the number of bolts over the width. The equations are taken from [34] and they apply to the net section stress.

The number of rows of bolts per side of the connection is denoted  $k$ . According to [35], the first row in connections with  $k > 1$  transfers a

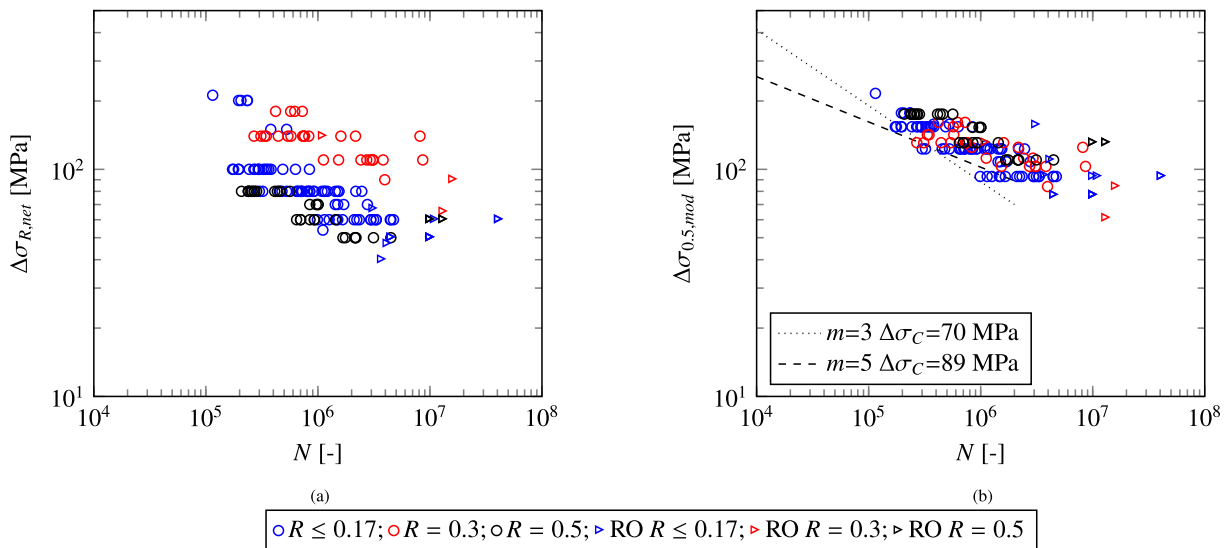


Fig. 4. Data for double covered connections (DCC) with non-preloaded bolts in normal clearance holes: (a) Net section stress; (b) Modified net section stress at  $R = 0.5$ .

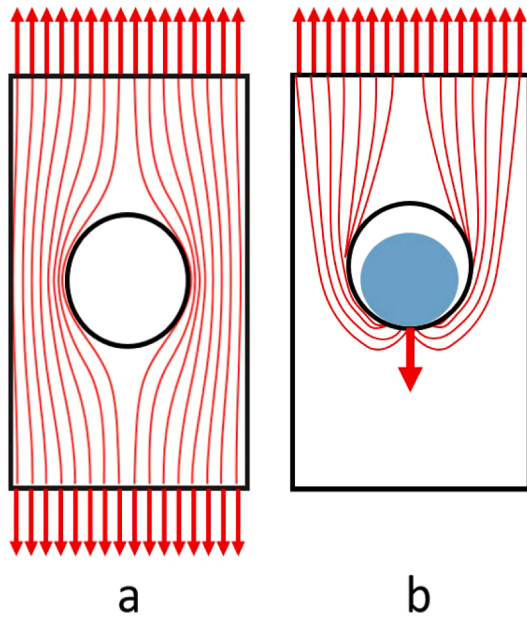


Fig. 5. Stress concentrations in DCC with non-preloaded bolts: (a) Bypass loading; (b) Pin loading.

slightly larger fraction of the force than the other rows, whereas [29] informs that each row takes an equal fraction. The latter approximation results into the following equation for the SCF at the first (decisive) bolt row:

$$K_t = \frac{1}{k}K_t^{pin} + \frac{k-1}{k}K_t^{byp} \tag{17}$$

Eq. (17) is simplified (with a coefficient of determination of 0.99 for the relevant range of  $0.05 \leq d_0/w \leq 0.5$ ) through:

$$K_t \approx c_1 + c_1 \left( c_2 - c_3 \frac{d_0}{w} \right)^3 \tag{18}$$

with coefficient  $c_1 = 2.55$  and coefficients  $c_2$  and  $c_3$  according to Table 2. The proposed stress range for evaluation of this detail type is:

$$\Delta\sigma_{R,mod} = \Delta\sigma_{R,net} \frac{K_t}{c_1} = \Delta\sigma_{R,net} \left( 1 + \left( c_2 - c_3 \frac{d_0}{w} \right)^3 \right) \tag{19}$$

Using data from individual series and geometries, the stress ratio effect was established as  $\xi = 0.5$ . Fig. 4(b) shows the data as a function of the modified stress range corrected to stress ratio  $R = 0.5$ . The significantly reduced scatter of the test data compared to Fig. 4(a) indicates that the newly defined stress range is an improvement over the net section stress range.

The data in Fig. 4 include HDG steel samples from [36] because the database excluding HDG steel is not large with 45 failed samples. The HDG steel series gave the same fatigue resistance as those of non-galvanized series with the same geometry and stress ratios in [36]. The fatigue reference resistance of the sub-group without HDG specimens is 1% higher than that of the entire database. A sub-group containing specimen with drilled holes in the plates gives a 5% higher fatigue reference resistance as compared to a sub-group of specimens

Table 2  
Coefficients  $c_2$  and  $c_3$  as a function of the number of bolt rows  $k$ .

$k$	1	2	$\geq 3$
$c_2$	1.6	1.3	1.1
$c_3$	2.7	2.2	1.8

Table 3  
Proposed FAT classes (constant amplitude fatigue limit at  $N = 2 \cdot 10^6$ ).

Detail	$m$	FAT	Stress calculation
A. DCC with preloaded bolts	5	112	Gross section
B1. Plates in non-preloaded DCC, drilled or reamed holes	5	90	Modified net section, Eq. (19) <sup>a)</sup>
B2. As B1, but punched or thermal cut holes	3	71	See B1
B3. Bolts in non-preloaded DCC	5	100	Average $\tau$ per shear plane <sup>b)</sup>
C. Single lap connection, preloaded bolts	5	100	Gross section <sup>c)</sup>
D1. Round holes drilled or reamed	5	90	Net section
D2. Round holes punched or thermal cut	3	50	Net section
E1. Bolt HT/R in tension	3	71	Tensile stress area <sup>d)</sup>
E2. Bolt R/HT in tension	3	56	See E1
E3. Bolt HDG or cut thread in tension	3	50	See E1

- a) With  $c_2$  and  $c_3$  of Table 2. Use  $k = 1$  for normal clearance holes.
- b) Thread not in shear plane. Use bolts of grade 5.6 or higher.
- c) Must be supported out of plane.
- d) Multiply FAT with Eq. (20) with  $\nu = 0.25$  for bolts with  $D > 30$  mm.

Table A.1  
DCC with preloaded bolts.

Source	$\sigma_y$ [MPa]	$\sigma_u$ [MPa]	$k$	$R$	$n$	$n_{RO}$
[10] <sup>a)</sup>	290	430	1	$-0.6 \leq R \leq 0.5$	89	22
[69] <sup>b)</sup>	280–470	?	2	0.1	80	0
[70]	286	?	1, 2 or 3	0.5	6	0
[71]	A588	?	1 or 2	0	20	0
[72]	372	490	2	$\approx 0.1$	1	5
[73]	A514	689	4	$\approx 0.25$	5	0
[37] <sup>c)</sup>	235–827	?	2 or 4	0	62	0
[31]	373	491	2 or 4	0	25	3

- a) Contains normal and HDG plates.
- b) Contains one series of weathering steel.
- c) Data of high strength steel ( $\sigma_y = 827$  MPa) only used for comparison.

Table A.2  
DCC with non-preloaded bolts in normal clearance holes, plate failure.

Source	$\sigma_y$ [MPa]	$\sigma_u$ [MPa]	Holes	$k$	$R$	$n$	$n_{RO}$
[10] <sup>a)</sup>	290	430	Drilled or punched	1	0.1 or 0.5	96	14
[74]	420	475	Drilled	2 or 3	0.3	27	4
[75]	224	431	Drilled	1	0	1	5
[76]	283	454	Drilled	2	0.15	1	0
[72]	372	490	Drilled or punched	1 or 2	$\approx 0.15$	6	0

- a) Contains normal and HDG plates.

with punched holes.

DCC with non-preloaded bolts in closely fitting holes – called fitted bolts hereafter – are also evaluated using Eq. (19), because the SCF-s of these detail types are similar. As the number of collected tests is small, data of old double covered hot-riveted connections are added to the data pool, but only those with red lead paint applied at the contact faces, as this results into a very low friction coefficient [37]. These riveted connections are expected to perform similarly as DCC with fitted bolts because of this low friction coefficient in combination with the generally low clamping force of rivets [38].

Table A.3 and Fig. 6 show the collected data. The slope parameter of the series with fitted bolts is  $\hat{m} = 4.1$ . The data have a stress ratio of  $0 \leq R \leq 0.25$ . The same stress ratio correction is applied as for non-preloaded bolts in normal clearance holes, i.e.  $\xi = 0.5$ . The fatigue resistance for the riveted connections is slightly below that of the fitted bolts. This may be related to heat treatment of the plate material during

**Table A.3**

DCC with non-preloaded fitted bolts or with rivets and red lead paint, plate failure.

Source	$\sigma_y$ [MPa]	$\sigma_u$ [MPa]	Type	$R$	$n$	$n_{RO}$
[77]	332	517	Fitted Bolts	0.05	5	1
[78]	440	605	Rivets	0.14	4	0
[79]	397–460	578–607	Rivets	0.11	8	2
[80]	(mild steel)	(mild steel)	Rivets	0.15	10	0

the riveting process, but it may also be related to the uncertainty in fatigue resistance associated with the small sample size. The number of series is too small to conclude whether the modified stress is a better predictor than the nominal stress for connections with fitted bolts. However, the fatigue resistance using the modified stress range is indeed almost equal to that of DCC with non-preloaded bolts in normal clearance holes in Fig. 4, which is in agreement with the theory of stress concentration.

The second failure mode of DCC with non-preloaded bolts is fatigue of the bolt loaded in shear. The stress range  $\Delta\tau_R$  is defined as the force range per shear plane divided either by the gross area of the bolt if the shear plane is in the non-threaded part, or by the stress area if the shear plane is in the threaded part. Only two sources are available, with data given in Table A.4 and Fig. 7. The figure demonstrates a very large influence of the shear plane location. For this reason, bolts with a shear plane through the threaded part should be avoided in such connections and the fatigue reference resistance in Fig. 7 is evaluated for the other data, i.e. source [39]. The slope parameter of the data in [39] is  $\hat{m} = 8$ . As only one series is available, the resulting fatigue resistance is compared to that of riveted connections failing through rivet shear in [40,41]. The resulting rivet fatigue resistance assuming  $m = 5$  is  $\Delta\sigma_C = 140$  MPa. This result is in line with that of the bolts:  $\Delta\sigma_C = 135$  MPa for the same slope.

All collected tests are carried out at relatively low stress ratios of  $R \approx 0.1$ . Davoli et al. [42] showed that the torsional fatigue resistance depends only slightly on the mean shear stress as long as the maximum shear stress does not exceed the static shear yield stress. Bennebach et al. [43] showed that the effect of the mean shear stress is larger in case of block loading with varying mean shear stress. However, both studies apply to a steel of much higher grade than those considered here. Most of the data of the other details, where components are loaded in tension, show a stress ratio effect that is on average  $\xi \approx 0.55$ . In the light of the references mentioned above, this stress ratio effect is probably

conservative for bolts loaded in shear with high stress ratio. If applied so, a conservative estimate of the fatigue reference resistance results of  $\Delta\sigma_C = 98$  MPa for  $m = 5$ .

It should be noted that this value is derived for DCC. The fatigue resistance may be lower in case of single lap connections because of the bending moment introduced in the bolts, but fatigue test data with this condition are not found. The bolts of series [39] are of grade 5.8. Bolts of higher grades are expected to have an equal or larger fatigue resistance. Lower strength bolts may have a lower fatigue resistance, but data are lacking. Lower strength bolts should hence not be used without substantiation of the fatigue resistance by tests.

### 3.3. Single lap connections with preloaded bolts

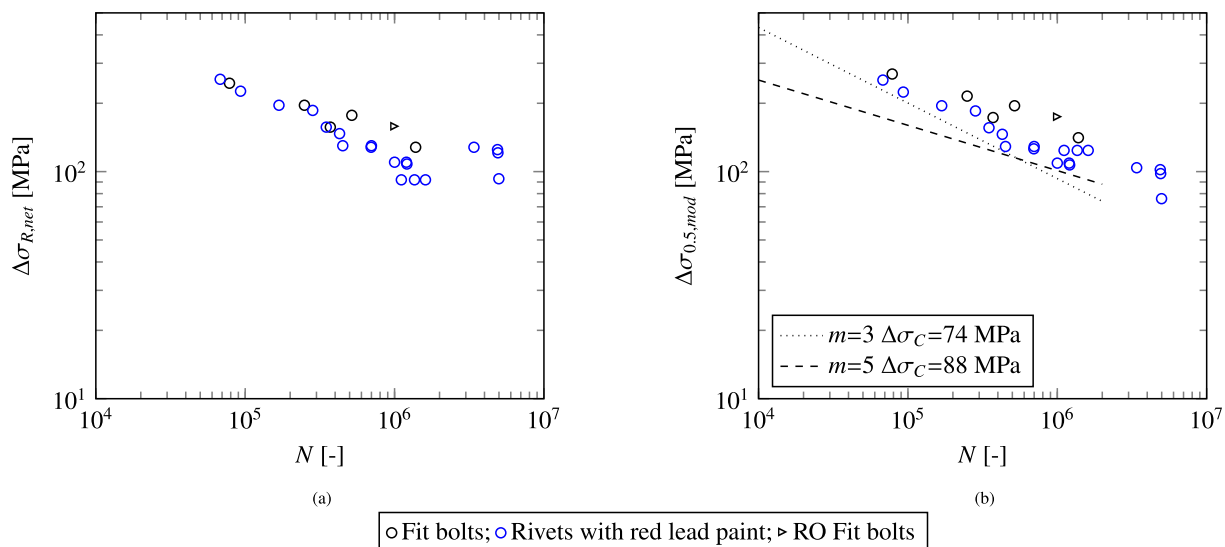
Single lap connections differ from DCC by having only one shear plane. Even when preloaded, these connections show a lower fatigue resistance than DCC, which is attributed to the unsymmetrical force distribution [30,37]. Single lap connections are often applied in situations where only a part of the cross-section is connected. This results into a geometry specific stress concentration [30], which should be determined on a case basis. Only data where the full cross-section is connected are used in the statistical evaluation.

Table A.5 and Fig. 8 present the data. The average values are  $\hat{m} = 3.7$  and  $\xi = 0.6$ . Approximately 50% of the data stem from [44], where the steel applied for plate and section material has been produced with the Thomas process. The possibly low fracture toughness of this type of steel may have influenced the fatigue performance. Although the Thomas process is no longer used, the data are still included because of demonstration purposes and because the number of other data is small. Fig. 8 shows a large scatter, even when considering only data from [44] for  $R = 0$ . One of the reasons for the large scatter is the difference in the support against out of plane deformation. To demonstrate this, Fig. 8 highlights two series from [44]:

**Table A.4**

DCC with non-preloaded bolts, bolt failure.

Source	Grade	shear plane	$R$	$n$	$n_{RO}$
[39]	5.8	plain	0.1	13	2
[31]	8.8–12.9	threaded	$0.1 \leq R \leq 0.35$	28	2



**Fig. 6.** Data for double covered connections (DCC) with fitted bolts or rivets: (a) Net section stress; (b) Modified net section stress at  $R = 0.5$ .

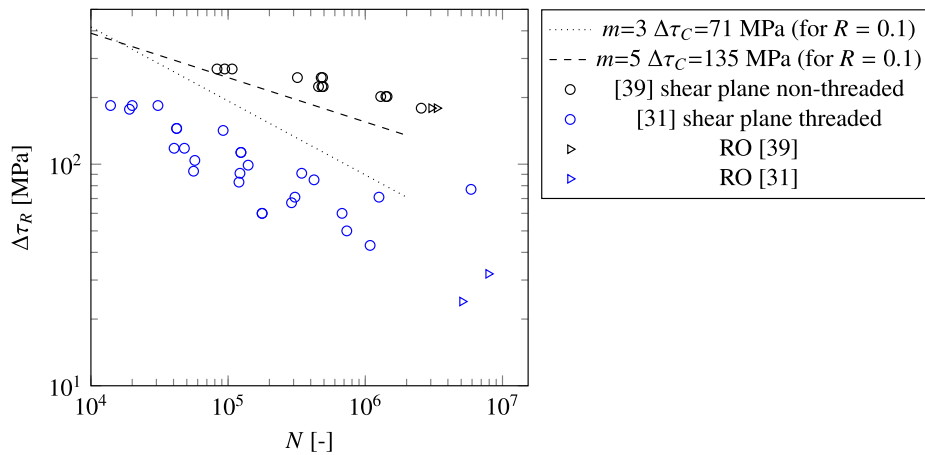


Fig. 7. Data for double covered connections (DCC) with bolt failure.

Table A.5  
Single lap connections with preloaded bolts.

Source	Grade	R	n	n <sub>RO</sub>
[81]	ASTM-A7	-1 ≤ R ≤ 0	30	0
[44] <sup>a)</sup>	Thomas	-1 ≤ R ≤ 0.1	36	4
[33] <sup>b)</sup>	Fe510	0.1	3	0

a) Only data with all connections fully supported are considered.  
b) Data from puddle iron specimens excluded.

- Series 1 has no lateral support. The distance between the grips in the test machine relative to the specimen cross-section was large. The fatigue resistance of this series is lower than that of the others.
- Series 2 (actually consisting of two geometries) has a full lateral support through the webs of the sections. The fatigue resistance of this series is higher than that of the others. The statistical evaluation

is performed only for series 2, giving a fatigue resistance of  $\Delta\sigma_C = 104$  MPa for  $m = 5$ .

The other series have a lateral support in between these two extreme cases and they have a fatigue resistance that is also in between, Fig. 8(b). Also for this type of connection [33] found that the fatigue resistance with preloaded injection bolts was lower than that of normal preloaded bolts.

### 3.4. Plates with holes

Many tests series are found for plates with holes, see Table A.6. Several sources such as [45] show that the fatigue resistance of plates with slotted holes is different from that of plates with round holes, in line with the expectation regarding the theoretical SCF. Only round holes are therefore considered. The fatigue resistance of plates with holes depends on the hole forming method, see e.g. [45,46]. Three methods are

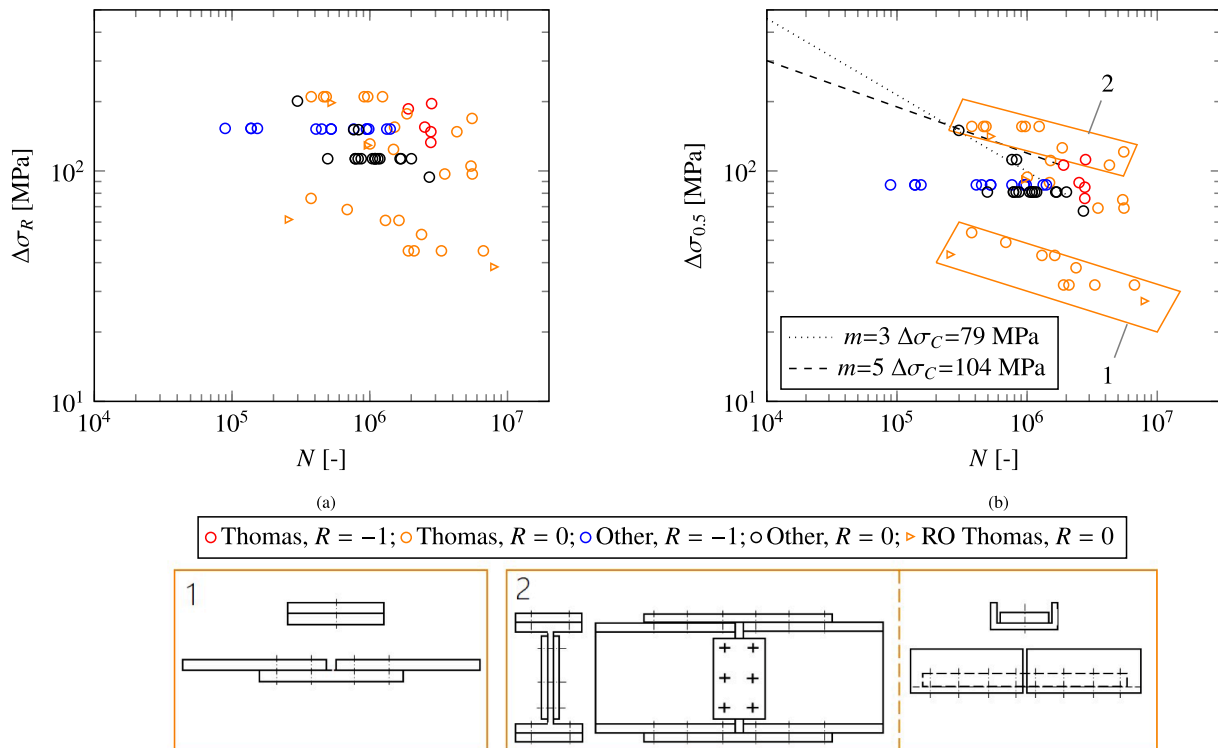


Fig. 8. Data for single lap connections with preloaded bolts: (a) As received; (b) Corrected to  $R = 0.5$ .

**Table A.6**  
Elements with a round hole.

Source	$\sigma_y$ [MPa]	$\sigma_u$ [MPa]	Hole forming	$R$	$n$	$n_{RO}$
[82] <sup>a</sup>	250–345 <sup>b</sup>	?	various	0.1	28	8
[83]	235–355 <sup>b</sup>	?	drilled	0.1	17	4
[84] <sup>c</sup>	235–355 <sup>b</sup>	?	drilled	0.1	16	3
[85]	235–390	396–641	drilled or reamed	0	47	8
[4]	427–484	559–596	thermal cut	0.1	65	25
[86]	359–538	511–596	drilled or punched	0.1	54	13
[79]	248–422	400–607	drilled	$0 \leq R \leq 0.28$	68	33
[87]	386	?	drilled	$-1 \leq R \leq 0.5$	29	9
[10]	235 <sup>b</sup>	?	drilled or punched	0.1	38	19
[88]	229–643	408–692	reamed	0	23	8
[89]	355–460 <sup>b</sup>	?	drilled or reamed	$-1 \leq R \leq 0.1$	134	0
[45]	355 <sup>b</sup>	?	drilled or oxy-fuel	0.1	45	2
[90]	355 <sup>b</sup>	?	drilled	$-1 \leq R \leq 0$	25	3

a) Data from HDG excluded.  
b) Nominal yield stress (no other data given).  
c) Staggered holes.

distinguished:

- Drilled holes, or holes that are reamed after any of the following two methods. Cracks initiate at the hole, near the centre of the plate thickness or at the plate surface for thick or thin plates, respectively.
- Thermally cut holes (Oxy-fuel, plasma or laser). These three methods appear to give a similar fatigue performance. The Vickers hardness was generally below 400 HV5.
- Punched holes. Cracks initiate at the hole at the plate surface [47].

Plates with waterjet cut holes as considered in [48] may have a higher fatigue resistance as compared to the three distinguished groups, but they are not considered here because waterjet cutting is seldomly applied in civil engineering structures. Data with different stress ratios were found for plates with drilled or reamed holes, Fig. 9(a), but most data are in the range  $0 \leq R \leq 0.1$ . A best fit of individual series is obtained by correcting for the stress ratio with  $\xi = 0.65$ . Fig. 9(b) shows that such a correction means that the data for  $0 \leq R \leq 0.1$  are on average below the

other data. This may be caused by local yielding at the hole edge at maximum stress in the first cycle(s) in the tests with high stress ratio. This has no effect on the stress range, but the effective stress ratio at the hole edge is then lower than the ratio of the externally applied load in the tests with high stress ratio. Hence, it may be conservative to correct the data for  $0 \leq R \leq 0.1$  to that of  $R = 0.5$ . The average slope parameter of the individual series is  $\hat{m} = 6.6$ . Using the net section stress range and assuming a slope parameter of  $m = 5$ , the fatigue reference resistance is 97 MPa.

Only data with  $0 \leq R \leq 0.1$  have been found for plates with thermally cut holes (except for one run-out at  $R = 0.5$ ) and punched holes. The data were corrected for the stress ratio by assuming the same correction factor as for drilled holes, i.e.  $\xi = 0.65$ , Fig. 10. The slope parameters of the individual series are  $\hat{m} = 3.7$  and 3.5 for thermally cut holes and punched holes, respectively. The steeper slopes and lower fatigue reference resistances of thermally cut or punched holes relative to drilled or reamed holes indicates the appropriateness of the subdivision into these groups.

A large range of plate and hole dimensions can be applied in practice, i.e. the variation in relative dimensions is larger than in case of the connections in the previous sections. The theoretical SCF, Eq. (15), suggests an influence of ratio  $d_0/w$ . The SCF further depends on the hole diameter over plate thickness ratio, evaluated in [49,50]. A fatigue notch factor can be derived from the theoretical SCF by considering the stress gradient near the notch according to [7]. Filippini [51] provides data for the stress gradient in plates with holes. It appears predominantly related to the ratio  $d_0^2/w$ . The fatigue notch factor of the test specimens is estimated from the equations or digitized figures in these sources. It is 2.16 on average, with a standard deviation of 0.08. Because of the low standard deviation, i.e. the similar geometries of the specimens, an evaluation using the notch stress per specimen did not give a noticeable lower scatter of the data, nor a different value for the fatigue reference resistance. The net section stress without modifications is therefore used in the evaluation, as this simplifies the evaluation for practice. BS 7608:2014 [3] provides an upper bound for the fatigue notch factor of 2.4 that should cover the majority of plate and hole dimension combinations in practice. The fatigue resistance may in such cases hence be about 10% lower as compared to the values in Figs. 9 and 10.

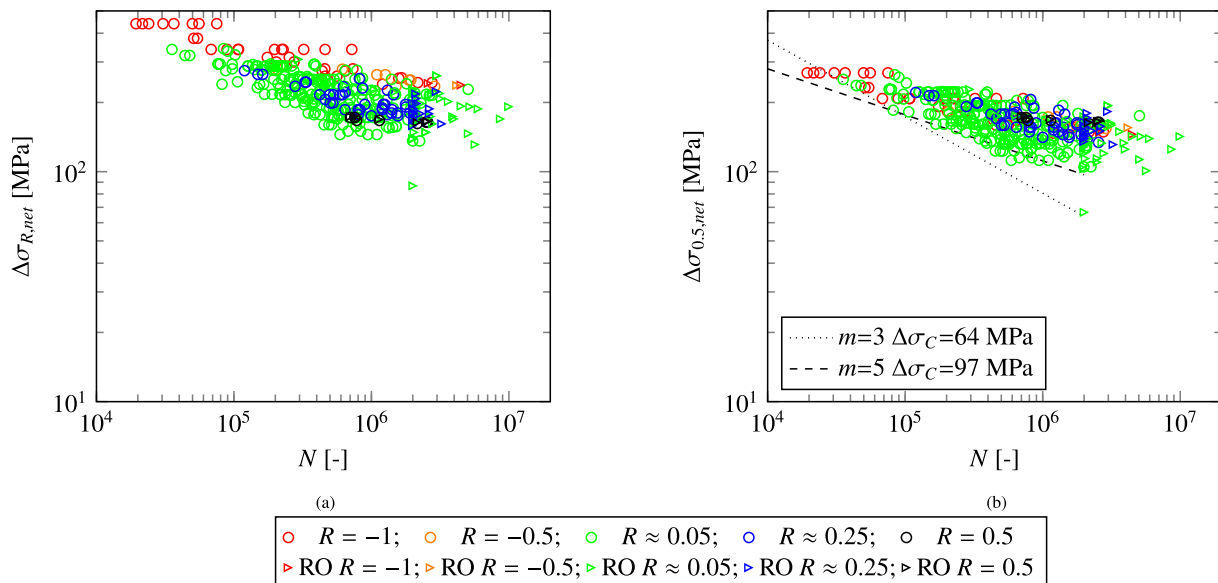


**Fig. 9.** Data for plates with drilled or reamed holes: (a) As received; (b) Corrected to  $R = 0.5$ .

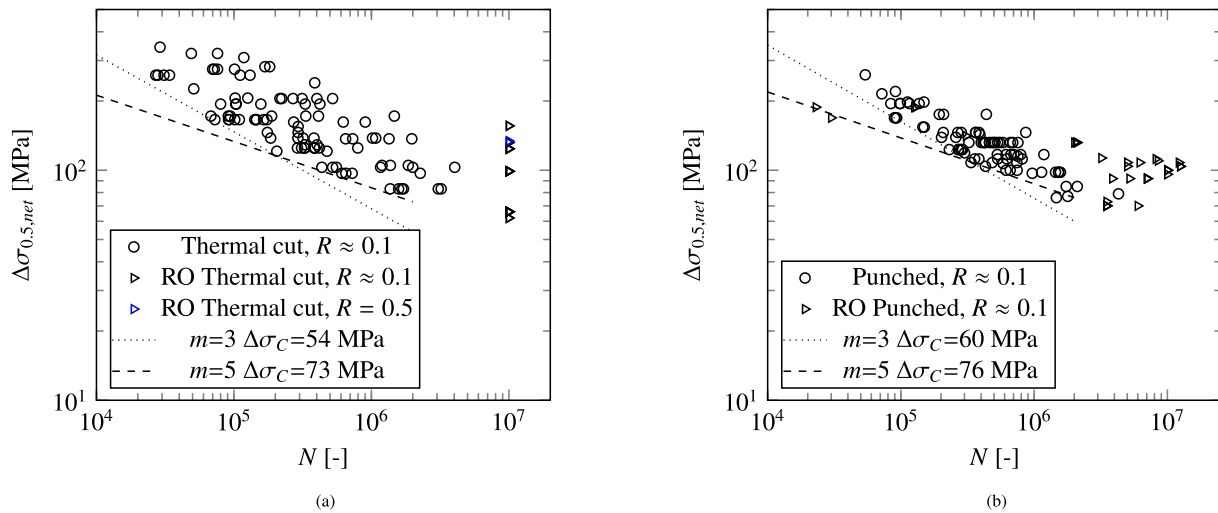


Fig. 10. Data for plates with holes, corrected to  $R = 0.5$ : (a) Thermally cut; (b) Punched.

3.5. Bolts loaded in tension

Bolts loaded in tension usually fail at the first thread in the nut, sometimes at the neck of the bolt head, and incidentally at the first thread adjacent to the unthreaded shank. The shape of the thread determines the stress concentration of the dominant failure mode. One of the consequences is that bolts with fine thread have a different fatigue resistance as compared to that of bolts with coarse thread. Civil engineering structures make almost exclusively use of bolts with ISO metric coarse thread [52]. For this reason, only bolts with that thread are evaluated.

Bolts loaded in tension are usually preloaded, as this significantly reduces the force range in the bolt. The fraction of the force range transferred through the bolt depends on the stiffness and composition of the plate assembly. Plates should be carefully leveled, as unintended prying effects due to imperfect plate assemblies may increase the force fraction in the bolt considerably [53]. Imperfections of plates are not considered in the evaluation below.

The nominal preload stress is usually equivalent to  $0.7\sigma_u$ . Table A.7 and Fig. 11 present the data on bolts loaded in tension, where a distinction is made between specimens with a high and with a low mean stress. The stress in this and in subsequent figures is defined as the force divided by the stress area of the bolt. The data of bolts with a low mean stress give on average a longer but also a more scattered fatigue life as compared to bolts with a high mean stress. The larger scatter is

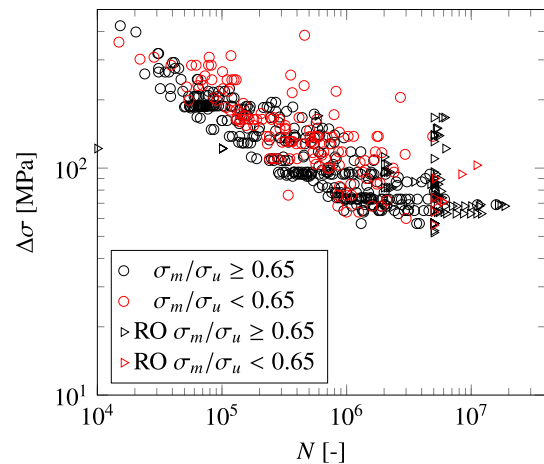


Fig. 11. Data for bolts in tension.

Table A.7  
Bolts in tension.

Source	Grade	Type	D [mm]	$\sigma_m/\sigma_u$	n	$n_{RO}$
[67]	8.8	R/HT	14	0.7	27	10
[91]	10.9	HDG	36	0.73	23	8
[92]	10.9	unknown	20	0.7	37	0
[57]	10.9, 12.9	HT/R	36–72	0.7	43	27
[31]	8.8, 12.9	HT/R, R/HT, Cut	12–36	0.25–0.55	57	4
[93]	10.9	R/HT	20	0.25–0.95	41	0
[94]	10.9	HDG	48	0.15	27	4
[95]	10.9	R/HT, HDG	36	0.7	50	17
[54]	10.9	R/HT, HDG	64	0.7	17	1
[64]	A36 A193 4340	HT/R, cut	35–51	0.3–0.6	32	4
[96]	10.9	R/HT	20	0.65	29	0
[97]	10.9	unknown	36	0.1–0.85	15	0
a)	10.9	R/HT, HDG	12–36	0.63	46	5

a) Personal correspondence with Fraunhofer LBF, Germany.

attributed to effects of imperfections. Strain measurements on bolts with a low preload in [31] demonstrate that the stress range is not equal around the perimeter of the bolt if that bolt is slightly crooked. Only the data with a mean stress  $> 0.6\sigma_u$  are considered hereafter.

Almost all specimens are of grade 8.8 or 10.9. The fatigue resistance of these two grades appears similar. The few specimens of lower grade suggest that lower grades give a slightly better fatigue performance. This is attributed to the lower mean stress in these bolts when preloaded to 70% of the tensile strength.

Subgroups are selected based on the following production methods, as they appear to influence the fatigue resistance:

- Heat treated and then hot-rolled bolts (HT/R). Such bolts may benefit from the compressive residual stresses caused by rolling at the crack initiation locations in the thread.
- Rolled and then heat treated bolts (R/HT).
- One of the previous methods, followed or preceded by Hot-Dip Galvanizing (HDG). Micro-cracking in the zinc layer may negatively affect the fatigue resistance [54].
- Bolts with cut thread (Cut). The potentially sharp thread geometry compared to rolling may negatively affect the fatigue resistance [55].

One of the consequence of the ISO course pitch metric thread is that the fatigue resistance depends on the bolt diameter. Different standards give different values for the bolt diameter influence. AASHTO [1] does not

specify a diameter influence. EN 1993-1-9 [2] and BS 6708 [3] give the following reduction on the fatigue resistance for bolt diameters  $D$  larger than 30 mm:

$$\Delta\sigma_C = \Delta\sigma_{C,M30} \left(\frac{30 \text{ mm}}{D}\right)^\nu \quad (20)$$

with  $\nu = 0.25$ . The guidelines in VDI 2230 [56] provide a smaller influence of the bolt diameter as compared to this equation. There is a growing interest from practice in large diameter bolts. Three sources of information are used here to evaluate the influence of the bolt diameter:

- Tests on HT/R bolts in [57] were carried out with bolt diameters ranging between  $36 \text{ mm} \leq D \leq 72 \text{ mm}$ . Assuming a slope parameter of  $m = 3$ , the mean fatigue resistance at 2 million cycles is determined for each bolt diameter. These are then compared. Tests on M36 and M64 R/HT bolts are evaluated in a similar way in [58]. These data are also considered.
- The theoretical SCF using nominal thread geometry is determined with the Finite Element Method (FEM). An axi-symmetrical model is made in software Abaqus v62.0, see Fig. 12(a) for the geometry and the mesh. Linear elements of type CAX4 are used for the elements and frictional contact is applied between the elements with a friction coefficient of 0.1, considered representative for lubricated bolts [59]. Such a model is not able to determine the exact value of the stress concentration because the gradual introduction of the first thread in the nut cannot be considered in such a model. However, it is expected that this method allows to compare SCF-s of different bolt diameters relative to each other. The SCF and the stress gradient resulting from the model are used to determine the fatigue notch factor,  $K_f$ , using [7].
- A crack growth calculation using a fracture mechanics (FM) model is carried out. Equations from [60] are used for the stress intensity factors, which are checked with results in [61]. A Paris equation with an exponent of 3 is used to determine the crack growth rate. An initial semi-circular (production) defect with a radius of 0.15 mm is assumed and the calculation is terminated after a crack depth of 0.6 times the bolt diameter is obtained. The calculation is used to estimate the ratios of the fatigue resistance considering crack growth for different diameters (hence the value of the Paris constant is not important).

Fig. 12(b) presents the results in terms of the predicted fatigue resistance relative to that of an M36 bolt. The fatigue notch factor and the FM calculations agree well with the test data of R/HT bolts [58] and these are in between VDI [56] and EN 1993-1-9 [2]. The data of HT/R bolts in [57], however, are generally below these models. The difference

between the evaluations using the mean resistance (open circles) or using the 95% exceedance fraction (filled circles) of that source demonstrates that the evaluation of the diameter effect is sensitive to the scatter in fatigue test data.

The thickness effect is also evaluated based on all fatigue test data, by assuming Eq. (20) for all bolt diameters (i.e. also for  $D < 30 \text{ mm}$ ) and fitting  $\nu$  such that  $s$  is minimized. Only results where failure occurred at  $N \leq 10^6$  cycles are considered in the fit, because the Basquin relation of Eq. (8) does not describe the data well for larger endurance. A best fit is obtained for  $\nu = 0.5, 0.15$  and  $0.05$  for the subgroups of HT/R, R/HT and HDG, respectively, but the evaluation is relatively insensitive to  $\nu$ . It should be mentioned that more data are available for the R/HT and HDG subgroups than for the HT/R subgroup. Because of this insensitivity and because of the different results for the different evaluation methods, the data are evaluated using the reduction according to EN 1993-1-9, which is expected to be generally conservative. Fig. 13 shows the result of this evaluation. Only few data are available for bolts with cut threads. Data of cut thread with  $\sigma_m/\sigma_u < 0.65$  confirm the general trend of the S-N curve and are all above the data shown.

Fig. 13 show a large difference in fatigue resistance between some of the subgroups, a relatively small standard deviation per subgroup, and a long transition from the finite to the near infinite life region. This gradual transition is also evident from the data on other details, but less pronounced as for bolts. The Basquin relation Eq. (8) does not describe the transition. For this reason, the data are also fitted with the Six Parameter Random Fatigue Limit Model (6PRFLM) [62], which is a random fatigue limit model based on [63]. Here, use is made of all data, including RO and failures at  $N > 10^6$  cycles. First step in the 6PRFLM is to estimate the fatigue limit  $\Delta\sigma_{lim}$ , which requires a sufficient number of run-outs at larger number of cycles than the failed data. For this reason, only data on HT/R and HDG bolts are fitted to the 6PRFLM. The 6PRFLM S-N curve reads:

$$\log N = \log a' - m' \log \Delta\sigma - p \log \left(1 - \frac{\Delta\sigma_{lim}}{\Delta\sigma}\right) \quad (21)$$

where the transition radius of the curve is controlled through parameter  $p$ . Parameters  $a'$  and  $m'$  have the same purpose as  $a$  and  $m$  in the Basquin relationship, but with different values. Leonetti et al. [62] explain how to obtain the distributions and the correlations of the parameters of the 6PRFLM. The 95% prediction bound is determined with Monte Carlo analysis using these distributions and correlations and assuming  $k_n = 1.64$ . It is plotted with continuous curves in Fig. 13. The figure shows that the slope parameter  $m'$  is close to 3 and that the 95% prediction bound of  $\Delta\sigma_{lim}$  is close to the value of  $\Delta\sigma_C$  of the Basquin relation for  $m = 3$ .

Threaded rods or stud bolts are not considered in the evaluation.

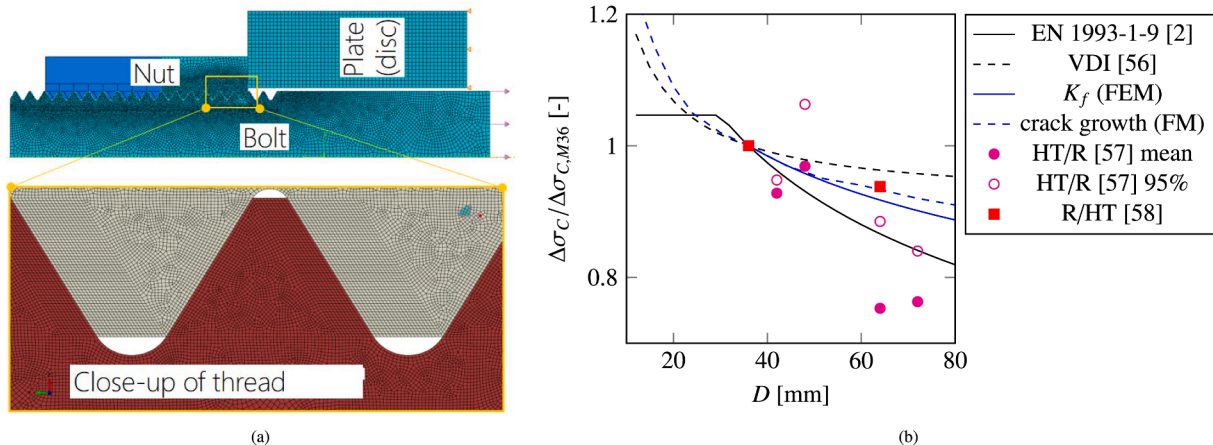


Fig. 12. Influence of bolt diameter on fatigue resistance: (a) Finite element model to determine the SCF; (b) fatigue resistance relative to that of an M36 bolt.

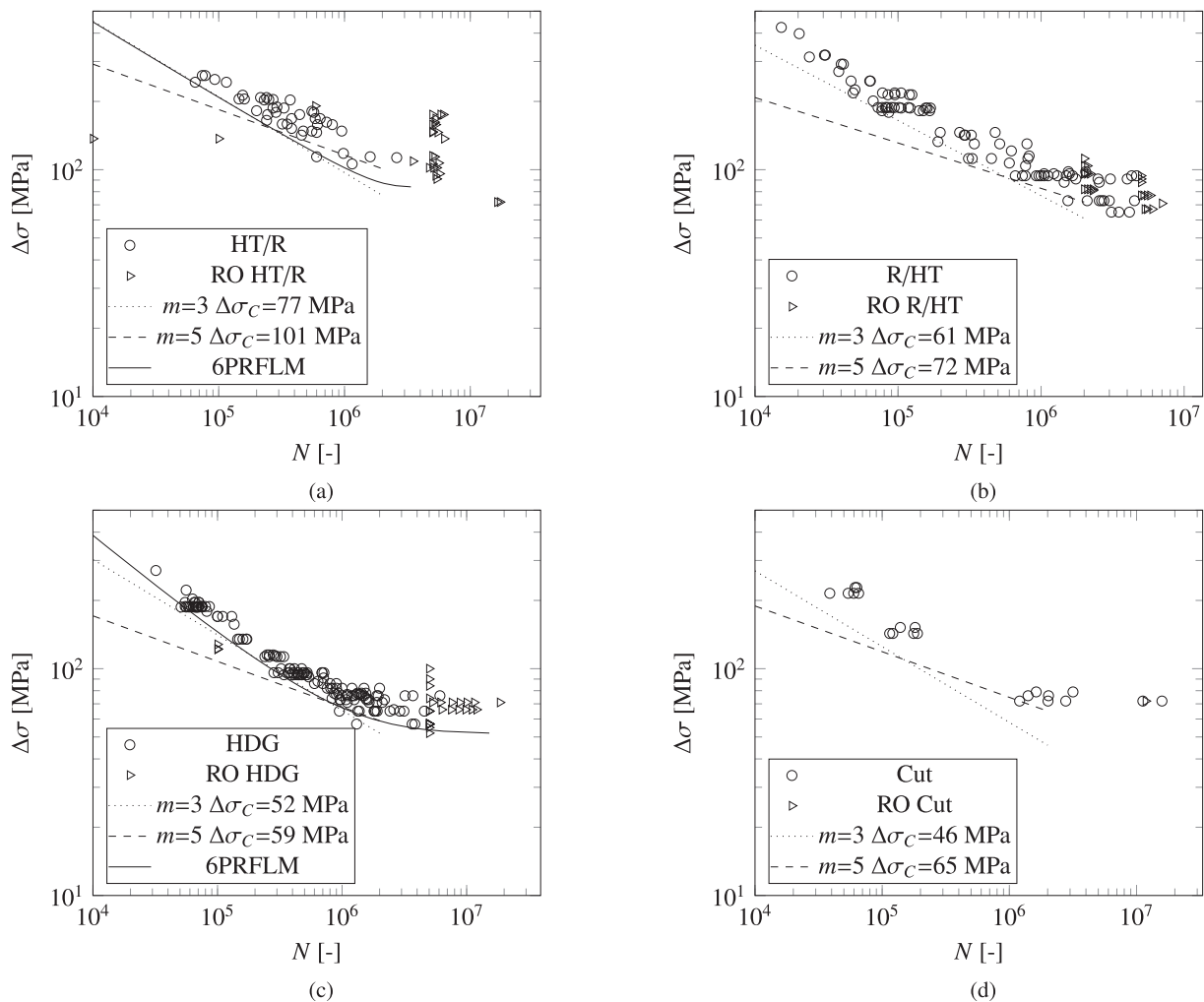


Fig. 13. Data for bolts in tension,  $\sigma_m/\sigma_u \geq 0.65$ , with diameter correction: (a) Heat treated then rolled (HT/R); (b) Rolled then heat treated (R/HT); (c) Galvanized (HDG); (d) Cut thread (Cut).

Data from American sources [64–66] on these elements show that the fatigue resistance is similar to that for bolts as presented above. It should be mentioned that the fatigue resistance of bolts or threaded rods loaded in bending is substantially larger than the tension case discussed here [67].

#### 4. Proposed FAT classes for the design

This section uses the evaluations of the previous section to propose FAT classes for the design of civil engineering structures. The lowest predefined FAT class in EN 1993-1-9 is 36 and each subsequent FAT class has a 12.5% higher fatigue resistance, rounded to integers. The FAT class is determined per detail as the fatigue reference resistance rounded down to the nearest predefined FAT class.

As explained, the fatigue reference resistance values are derived for steel grades with a nominal yield stress up to 460 MPa. Test data on higher strength details appear to generally give equal or higher fatigue endurance. The FAT classes derived can therefore be conservatively applied to higher grade steels, within the general bounds set by the Eurocode (grades up to S960).

A few judgement choices have been made:

- Generally, details with a longer fatigue initiation life and a higher fatigue resistance have a larger slope parameter. This is confirmed by the slope estimate per series in the previous section. The slope

parameter per detail is selected based on this generality as either  $m = 3$  or  $m = 5$ .

- Plates with drilled or reamed holes gave a higher fatigue resistance and a higher slope parameter than plates with thermally cut or punched holes. Although a smaller difference between these hole forming methods was observed for net section failure in DCC with non-preloaded bolts, the same distinction in hole forming method is made for these connections, as a conservative approximation.
- Assuming a slope  $m = 5$ , Section 3.1 shows that the fatigue resistance of DCC with preloaded bolts increases when omitting tests carried out with very high maximum stress and it approaches (but does not reach) the resistance associated to a free slope ( $\Delta\sigma_C = 112$  MPa). Given the relevancy in practice of small stress ranges and high endurance, it is therefore reasonable to adopt FAT class 112.
- Sections 3.1 and 3.3 suggest that plate failure in connections with preloaded injection bolts give a lower fatigue resistance than connections with preloaded high strength friction grip bolts (without injection). However, this is based on only one source. The FAT class of connections with preloaded injection bolts is therefore not yet established.
- Imperfections in the alignment of holes in the different plates of a DCC with bolts may occur. If not preloaded, this may imply that not all bolts participate in transferring the fatigue force. For this reason, it is suggested that only one bolt row ( $k = 1$ ) is considered in the calculation of the stress with Eq. (19). Such a situation is less likely

for fitted bolts, as the holes are then made in the entire plate assembly at once.

- Rounding down to the nearest FAT class implies for plates with holes that some allowance is available for the difference in fatigue notch factor between the tests and the practical upper bound, Section 3.4.
- Failures are observed at very large numbers of cycles, but a gradual transition is observed between the finite and the near infinite regions. Using the Basquin relation with the 95% prediction bound, no single failure was observed below  $\Delta\sigma_C$  (at two million cycles) and only very few below the Basquin relation at one million cycles. The 6PRFLM applied to bolts confirmed that the near infinite life coincides with  $\Delta\sigma_C$ . This applies to plates and bolts loaded in tension. Tests in [68] on smooth and scratched specimens loaded in shear also show a transition at about one or two million cycles. For design practice, a constant amplitude fatigue limit may thus be assumed at two million cycles.

The authors do not claim to have accounted for all influencing factors on the fatigue resistance per detail type. However, it is expected that the dominant influencing factors are considered, which allows for an appropriate selection of the FAT class per detail. Table 3 gives these recommended FAT classes. These have been implemented in the revised version of EN 1993-1-9 that is sent to the European member states for commentary.

## 5. Conclusions

The evaluation of a large number of fatigue tests on bolts and bolted connections with production qualities and dimensions relevant for civil engineering structures have revealed the possibility to improve current design specifications. These have been implemented in the revision of the European standard EN 1993-1-9.

- Most details benefit from sub-grouping into separate FAT classes based on the production process, such as the hole forming method in plates or the thread forming method of bolts.
- Most details show a gradual transition from the finite life to the near infinite life regions of the S-N curve. The Basquin relation is therefore less suited to describe the data, but it is still proposed for the new generation of EN 1993-1-9 because of its ease in use. Using the Basquin relation, the near infinite life region commences at approximately one or two million cycles for the details considered.
- A substantial influence of the stress ratio,  $R$ , is observed. Expressing the fatigue resistance at stress ratio  $R$  relative to that at  $R = 0$  with the factor  $(1 - R)/(1 - \xi R)$ , the values of  $\xi$  established per detail and range between  $0.4 \leq \xi \leq 0.65$  for the fatigue test data ranging between  $-1 \leq R \leq 0.5$ . The FAT classes are derived for  $R = 0.5$ .
- Most fatigue tests are carried out at  $0 \leq R \leq 0.1$ . It is recommended to carry out more tests at higher stress ratios to substantiate the stress ratio influence. More data would also be welcome to establish the size effect of bolts that are heat treated and then rolled.
- Yielding has an important influence on DCC with preloaded bolts. The FAT class should be based on data where yielding has not taken place.
- The stress calculation in Double Covered Connections (DCC) with non-preloaded bolts should be based on the stress concentration at the hole edge. The net section stress is not appropriate for this detail. A simple design equation is proposed.

## Declaration of Competing Interest

The authors declare that they have no known competing financial interests or personal relationships that could have appeared to influence the work reported in this paper.

## Acknowledgements

The members of the experts committees ECCS-TC6 and CEN/TC250/SC3/WG9 are acknowledged for the discussions about the evaluation. Helen Bartsch (RWTH Aachen), Sjors van Es (TNO) and Richard Pijpers (TNO) are acknowledged for collecting a number of sources with fatigue test data. Matthijs Bakker (TNO) is acknowledged for producing the finite element model of bolts. This work has not received funding.

## Appendix A. Description of the test series

This appendix gives the description of the test series and the used sources per detail type.

## References

- [1] AASHTO:2012. AASHTO LRFD Bridge Design Specifications. American Association of State Highway and Transportation Officials; 2012.
- [2] EN 1993-1-9:2005. Eurocode 3: Design of steel structures - Part 1-9: Fatigue. CEN; 2005.
- [3] BS 7608:2014. Guide to fatigue design and assessment of steel products. BSI; 2014.
- [4] Cicero S, García T, Álvarez JA, Martín-Meizoso A, Aldazabal J, Bannister A, et al. Definition and validation of eurocode 3 fat classes for structural steels containing oxy-fuel, plasma and laser cut holes. *Int J Fatigue* 2016;87:50–8.
- [5] Cicero S, García T, Álvarez JA, Bannister A, Klimpel A, Martín-Meizoso A, et al. Fatigue behaviour of structural steels with oxy-fuel, plasma and laser cut straight edges. definition of eurocode 3 fat classes. *Eng Struct* 2016;111:152–61.
- [6] Gurney TR. Fatigue of welded structures. Cambridge University Press; 1979.
- [7] FKM:2001. Rechnerischer Festigkeitsnachweis für Maschinenbauteile. VDMA Verlag GmbH; 2012.
- [8] Ferraz G, Rossi B. On the fatigue behaviour of hot dip galvanized structural steel details. *Eng Fail Anal* 2020;118:104834.
- [9] Bergengren Y, Melander A. An experimental and theoretical study of the fatigue properties of hot-dip galvanized high strength sheet steel. *Int J Fatigue* 1992;14:154–62.
- [10] Valtinat G, Huhn H. Betriebsfestigkeit von stählernen Lochstäben und Schraubenverbindungen mit feuerverzinkten Bauteilen und gestanzten Löchern. Düsseldorf: Gemeinschaftsausschuß Verzinken; 2000.
- [11] Nilsson T, Engberg G, Trogen H. Fatigue properties of hot-dip galvanized steels. *Scand J Metall* 1989;18:166–75.
- [12] Vogt JB, Boussac O, Foct J. Prediction of fatigue resistance of a hot-dip galvanized steel. *Fatigue Fract Eng Mater Struct* 2000;23:33–9.
- [13] Mischke CR. Prediction of stochastic endurance strength. *J Vib Acoust Stress Reliab* 1987;109:113–22.
- [14] DB-Richtlinie 805:2002. Tragsicherheit bestehender Eisenbahnbrücken. Deutsche Bahn; 2002.
- [15] Soderberg C. Factor of safety and working stress. *Trans ASME* 1939;52:13–28.
- [16] Goodman J. Mechanics applied to engineering. first ed. London: Longmans Green and Co; 1899.
- [17] Walker K. The effect of stress ratio during crack propagation and fatigue for 2024-t3 and 7075-t6 aluminum. In: Effects of Environment and Complex Load History on Fatigue Life, ASTM STP 462. American Society for Testing and Materials; 1970. p. 1–14.
- [18] Smith KN, Watson P, Topper TH. Stress-strain function for the fatigue of metals. *J Mater* 1970;5:767–78.
- [19] Langlais TE, Vogel JH. Overcoming limitations of the conventional strain-life fatigue damage model. *J Eng Mater Technol* 1995;117:103–8.
- [20] Gerber W. Bestimmung der zulässigen Spannungen in Eisen-Constructionen. *Z Bayer Archit Ing Ver* 1874;6:101–10.
- [21] Dietmann H. Festigkeitsberechnung bei mehrachsiger Schwingbeanspruchung. *Konstruktion* 1973;25:181–9.
- [22] Marin J. Interpretation of fatigue strength for combined stresses. In: Proceedings of international conference on fatigue of metals, institution of mechanical engineers; 1956. p. 184–94.
- [23] Schneider CRA, Maddox SJ. Best practice guide on statistical analysis of fatigue data. TWI doc. 13604.01/02/1157.02. The Welding Institute; 2002.
- [24] Stephens MA. Edf statistics for goodness of fit and some comparisons. *J Am Stat Assoc* 1973;69:730–7.
- [25] Jimenez-Pena C, Talemi RH, Rossi B, Debruyne D. Investigations on the fretting fatigue failure mechanism of bolted joints in high strength steel subjected to different levels of pretension. *Tribol Int* 2016;108:128–40.
- [26] Juoksukangas J, Lehtovaara A, Mantyla A. Experimental and numerical investigation of fretting fatigue behaviour in bolted joints. *Tribol Int* 2016;103:440–8.
- [27] Zampieri P, Curtarello A, Maiorana E, Pellegrino C. A review of the fatigue strength of shear bolted connections. *Int J Steel Struct* 2019;19:1084–98.
- [28] Wattar F, Albrecht P, Sahli AH. End-bolted cover plates. *J Struct Eng* 1985;111:1235–49.
- [29] Yin WS, Fang QH, Wang SX, Wang XH. Fatigue strength of high strength bolted joints. In: Proceedings of 3th IABSE congress. IABSE; 1982. p. 707–14.

- [30] Albrecht P, Mecklenburg MF, Evans BM. Fatigue strength of bolted joints. *J Struct Eng* 1987;113:1834–49.
- [31] [no names], Fatigue tests on steel bolts, report OTO 97067. Health and Safety Executive; 1998.
- [32] Bouwman LP, Gresnigt AM. Design of connections with injection bolts. Delft University of Technology; 1989.
- [33] Correia JAFO, Pedrosa BAS, Raposo PC, De Jesus AMP, Santos Gervásio HM, Lesiuk GS, et al. Fatigue strength evaluation of resin-injected bolted connections using statistical analysis. *Engineering* 2017;3:795–805.
- [34] Pilkey WD, Pilkey DF. Peterson's Stress Concentration Factors. 3rd ed. Wiley; 2008.
- [35] Martin ST. Load distribution in bolted joints. Lehigh University 1960.
- [36] Valtinat G, Huhn H. Festigkeitssteigerung von Schraubenverbindungen bei ermüdungsbeanspruchten, feuerverzinkten Stahlkonstruktionen. *Stahlbau* 2003; 72:715–24.
- [37] Kulak GL, Fisher JW, Struik JHA. Guide to Design Criteria for Bolted and Riveted joints. 2nd ed. American Institute of Steel Construction (AISC); 2001.
- [38] Leonetti D, Maljaars J, Pasquarelli G, Brando G. Rivet clamping force of as-built hot-riveted connections in steel bridges. *J Constr Steel Res* 2020;167:105955.
- [39] Wichtowski B. Untersuchungen zur Ermüdungsfestigkeit von Paßschrauben beim Abscheren. *Stahlbau* 2007;76:235–40.
- [40] Brühwiler E, Hirt MA. Das Ermüdungsverhalten genieteter Brückenbauteile. *Stahlbau* 1987;56:1–8.
- [41] Pipinato A, Pellegrino C, Bursi OS, Modena C. High-cycle fatigue behavior of riveted connections for railway metal bridges. *J Constr Steel Res* 2009;65:2167–75.
- [42] Davoli P, Bernasconi A, Filippini M, Foletti S, Papadopoulos IV. Independence of the torsional fatigue limit upon a mean shear stress. *Int J Fatigue* 2003;25:471–80.
- [43] Bennebach M, Palin-Luc T, Messenger A. Effect of mean shear stress on the fatigue strength of notched components under multiaxial stress state. *Procedia Eng* 2018; 213:25–35.
- [44] Klöppel K, Seeger T. Dauerversuche mit einschneidigen HV-Verbindungen aus St 37. *Stahlbau* 1964;33:225–45.
- [45] Mang F, Klingler J, Bucak O. Untersuchung der Dauerfestigkeit von Proben aus Stahl mit brenngeschnittenen Löchern. Schweißen und Schneiden 1989;41:81–5.
- [46] Sanchez L, Gutiérrez-Solana F, Pesquera D. Fatigue behaviour of punched structural plates. *Eng Fail Anal* 2004;11:751–64.
- [47] Alegre JM, Gutiérrez-Solana F, Aragón A. A finite element simulation methodology of the fatigue behaviour of punched and drilled plate components. *Eng Fail Anal* 2004;11:737–50.
- [48] Caiza P, Ummenhofer T. A probabilistic stüssi function for modelling the s-n curves and its application on specimens made of steel s355j2+n. *Int J Fatigue* 2018;117: 121–34.
- [49] Yu P, Guo W, She C, Zhao J. The influence of poisson's ratio on thickness-dependent stress concentration at elliptical holes in elastic plates. *Int J Fatigue* 2008; 30:165–71.
- [50] Yang Z, Kim CB, Cho C, Beom HG. The concentration of stress and strain in finite thickness elastic plate containing a circular hole. *Int J Solids Struct* 2008;45: 713–31.
- [51] Filippini M. Stress gradient calculations at notches. *Int J Fatigue* 2000;22:397–409.
- [52] ISO 965-1:2013. General purpose metric screw threads - Tolerances - Part 1: Principles and basic data. ISO; 2013.
- [53] Piraprez E. The effect of prying stress ranges on fatigue behaviour of bolted connections: The state-of-the-art. *J Constr Steel Res* 1993;27:55–68.
- [54] Schaumann P, Eichstädt R, Oechsner M, Simonsen F. Experimental fatigue assessment of high-strength bolts with large diameters in consideration of boundary layer effects. In: METEC and 2nd ESTAD 2015, Düsseldorf; 2015.
- [55] Unglaub J, Reininghaus M, Thiele K. Zur Ermüdungsfestigkeit von feuerverzinkten Zugstäben mit Endgewinden. *Stahlbau* 2015;84:584–8.
- [56] VDI 2230:2015. Systematic calculation of highly stresses bolted joints. VDI; 2015.
- [57] Hanenkamp W. Untersuchungen zur Zeit- und Dauerfestigkeit von Hochfesten Schraubenbolzen (10.9) im Durchmesserbereich M36 bis M72. *Konstruktion* 1992; 44:255–60.
- [58] Schaumann P, Eichstädt R. Ermüdung sehr großer HV-Schraubengarnituren. *Stahlbau* 2016;85:604–11.
- [59] Van Beek A. Advanced Engineering Design - Lifetime Performance and Reliability. TU Delft; 2019.
- [60] James L, Mills W. Review and synthesis of stress intensity factor solutions applicable to cracks in bolts. *Eng Fract Mech* 1988;30:641–54.
- [61] Korin I, Perez Ipiña J. Experimental evaluation of fatigue life and fatigue crack growth in a tension bolt-nut threaded connection. *Int J Fatigue* 2001;33:166–75.
- [62] Leonetti D, Maljaars J, Snijder HH. Fitting fatigue test data with a novel s-n curve using frequentist and bayesian inference. *Int J Fatigue* 2017;105:128–43.
- [63] Pascual FG, Meeker WQ. Estimating fatigue curves with the random fatigue limit model. *Technometrics* 1999;41:277–89.
- [64] Fischer F, Frank K. Axial tension fatigue strength of anchor bolts. University of Texas; 1977.
- [65] Frank K. Fatigue strength of anchor bolts. *J Struct Div* 1980;106:1279–93.
- [66] Van Dien JP, Kaczinski MR, Dexter RJ. Fatigue testing of anchor bolts. In: Proceedings of the 14th Structures congress. ASCE; 1996. p. 337–44.
- [67] Wentzel H, Huang X. Experimental characterization of the bending fatigue strength of threaded fasteners. *Int J Fatigue* 2015;72:102–8.
- [68] Nishimura Y, Yanase K, Tanaka Y, Miyamoto N, Miyakawa S, Endo M. Effects of mean shear stress on the torsional fatigue strength of a spring steel with small scratches. *Int J Damage Mech* 2020;29:4–18.
- [69] Lieurance HP. Etude de la tenue à la fatigue des assemblages boulonnés en aciers à haute limite d'élasticité. IRSID; 1976.
- [70] Mas E, Janss J. Assemblages par boulons à haute résistance - Fatigue des assemblages à double couvre-joint. CRIF; 1964.
- [71] Albrecht P, Mecklenburg MF, Evans BM. Screening of structural adhesives for application to steel bridges. US Department of Transportation, Federal Highway Administration; 1985.
- [72] Brown JD. Punched Holes in Structural Connections, Dissertation at The University of Texas, Austin; 2006.
- [73] Frank KH, Yura JA. An experimental study of bolted shear connections. Austin: University of Texas; 1981.
- [74] Josi G, Grondin GY, Kulak GL. Fatigue of Bearing-type Shear Splice. University of Alberta, Department of Civil and Environmental Engineering; 1999.
- [75] Wilson WM, Thomas FP. Fatigue tests of riveted joints. University of Illinois; 1938.
- [76] Steinhart O, Möhler K. Versuche zur Anwendung vorgespannter Schrauben im Stahlbau – I. Teil, Berichte des Deutschen Ausschusses für. *Stahlbau* 1954;18.
- [77] Graf O. Versuche mit Schraubenverbindungen, Berichte des Deutschen Ausschusses für. *Stahlbau* 1951;16:1–19.
- [78] Graf O. Versuche im Stahlbau - Dauerversuche mit Nietverbindungen. Berichte des Deutschen Ausschusses für Stahlbau 1935;5:1–61.
- [79] Klöppel K. Gemeinschaftsversuche zur Bestimmung der Schwellzugfestigkeit voller, gelochter und genieteter Stäbe aus St37 und St52. *Bautechnik* 1936;13(14): 96–112.
- [80] [no names], Statistische Auswertung von Ermüdungsversuchen an Nietverbindungen in Flussstahl. Office de Recherches et d'Essais. Union Internationale des Chemins de fer (ORE UIC); 1986.
- [81] Munse W, Wright D, Newmark N. Laboratory tests of high tensile bolted structural joints. *Trans ASCE* 1954;80:1.
- [82] Brown JD, Lubitz DJ, Cekov YC, Frank KH, Keating PB. Evaluation of Influence of Hole Making upon the Performance of Structural Steel Plates and Connections. University of Texas; 2007.
- [83] Steinhart O, Möhler K. Versuche zur Anwendung vorgespannter Schrauben im Stahlbau – II. Teil, Berichte des Deutschen Ausschusses für. *Stahlbau* 1959;22.
- [84] Steinhart O, Möhler K. Versuche zur Anwendung vorgespannter Schrauben im Stahlbau – III. Teil, Berichte des Deutschen Ausschusses für. *Stahlbau* 1962;22.
- [85] Hansen NG. Fatigue tests of high-strength steel. *Trans ASCE* 1961;126:750–63.
- [86] Bannister AC, Skalidakis M, Pariser A, Langenberg P, Gutierrez-Solana F, Sánchez L, et al. Performance criteria for cold formed structural steels. European Commission; 2006.
- [87] Klöppel K. Dauerfestigkeitsversuche mit Schweissverbindungen aus St 52, *Stahlbau* 1960; 1960. p-p.
- [88] Gurney T. Some exploratory fatigue tests on notched mild and high tensile steels. *Brit Weld J* 1964;1964:457–61.
- [89] [no names], EUR 5357 e, 1975. European Commission; 1975.
- [90] Berto F, Mutignani F, Tisalvi M. Notch effect on the fatigue behaviour of a hot-dip galvanized structural steel. *Strength Mater* 2015;47:719–27.
- [91] Berger C, Schaumann P, Stolle C, Marten F. Fatigue strength of high strength bolts with large diameters (Ermüdungsfestigkeit hochfester Schrauben großer Abmessungen). Zentrum für Konstruktionswerkstoffe, Technische Universität Darmstadt; 2008.
- [92] Bouwman LP. Fatigue of Bolted Connections and Bolts Loaded in Tension. Stevin Laboratory, Delft University of Technology; 1979.
- [93] Kuperus A. Fatigue Tests on Tensile Loaded High Strength Bolts and Studbolts. ECCS/Delft University of Technology; 1971.
- [94] Marten F. Zur Ermüdungsfestigkeit hochfester großer Schrauben. Institut für Stahlbau, Universität Hannover; 2009.
- [95] Schaumann P, Eichstädt R. Fatigue assessment of high-strength bolts with very large diameters in substructures for offshore wind turbines, in: Proc. In: 25th Int. Ocean Polar Engng Conf (ISOPE). ISOPE; 2015. p. 260–7.
- [96] Lacher G. Zeit- und Dauerfestigkeit von schwarzen und feuerverzinkten hochfesten Schrauben M20 der Festigkeitsklasse 10.9 unter axialer Beanspruchung. Bauingenieur 1986;61:227–33.
- [97] Mang F, Herion S, Fleischer O, Koch E. Untersuchung von Zug-Druck-Kalottenlagern im Großversuch. *Stahlbau* 2003;72:43–9.